Rotational dynamics of C_{60}^{4-} and electronic excitation in Rb_4C_{60}

G. Zimmer and M. Mehring
2. Physikalisches Institut, Universität Stuttgart, 70550 Stuttgart, Federal Republic of Germany

C. Goze and F. Rachdi
Groupe de Dynamique des Phases Condensées, Université Montpellier II, 34095 Montpellier, France
(Received 30 January 1995; revised manuscript received 2 June 1995)

10% ^{13}C enriched Rb_4C_{60} was investigated by ^{13}C NMR. The relaxation rates T_1^{-1} and T_2^{-1} are basically determined by reorientation of the C_{60}^{4-} molecules. In addition, T_1^{-1} exhibits an activated electronic contribution with activation energy 104 meV. The same activation energy is also found in Knight-shift measurements. Both compounds, Rb_4C_{60} and K_4C_{60}, exhibit the same electronic excitation with the same activation energy within experimental error. We attribute this to a local excitation into a high-spin state of the Jahn-Teller distorted C_{60}^{4-}.

I. INTRODUCTION

The phase diagram of the known stable phases A_xC_{60} (A=K, Rb) shows a rather rich variety in the physical properties: In A_1C_{60} polymerization and one-dimensional solid-state properties were proposed,[1] the A_3C_{60} compounds are known to be superconductors, whereas the insulating A_6C_{60} compounds show diamagnetic behavior.[2] The A_4C_{60} series has been the subject of some recent experimental investigations,[3–5] concerning its electronic properties: Murphy *et al.* found in ^{13}C NMR experiments a line shift of 182 ppm for Rb_4C_{60},[6] Ruani *et al.* deduce an electronic activation energy of 50 meV from Raman measurements,[7] whereas ^{13}C NMR data on K_4C_{60} revealed a value of 104 meV.[8] μSR experiments on K_4C_{60} show an energy gap of 300 meV,[9] which leads to a semiconductor model for A_4C_{60}. Another interesting point is the C_{60}^{4-} molecular dynamics[8] which is supposed to depend on the alkali counterion. We will address this point here by applying relaxation (T_1^{-1},T_2^{-1}) measurements.

In this contribution we report on the temperature-dependent ^{13}C shift as well as relaxation measurements of a 10% ^{13}C enriched Rb_4C_{60} sample. The results will be compared with those obtained from a K_4C_{60} sample with natural abundant ^{13}C. The paper is organized as follows. After a brief description of the sample preparation, the experimental setup and NMR procedures applied as well as the parameters used in this investigation (Sec. II), the results will be presented and discussed in Sec. III. We will differentiate between shift measurements (Sec. III A), T_1 relaxation caused by molecular reorientation (Sec. III B), and electronic excitations (Sec. III C). The temperature-dependent linewidth and T_2 measurements will be discussed in Sec. III D.

II. EXPERIMENT

The nominal Rb_4C_{60} sample was prepared by vapor doping similar to the procedure outlined in Refs. 10–12 and was characterized by ^{13}C MAS NMR (45.6 MHz) as well as x ray, revealing about 83% of the sample in the Rb_4C_{60} phase with 17% contamination from Rb_6C_{60}. It should be noted here that ^{13}C MAS NMR is very sensitive in detecting small clusters of unwanted phases which might escape detection by x rays. ^{13}C MAS NMR of Rb_4C_{60} shows at room temperature a 1–2 ppm broad line in agreement with a rapid rotation of the C_{60}^{4-} molecules in the Rb_4C_{60} phase. The Rb_6C_{60} impurity phase does not influence the ^{13}C measurements shown below because of the about 60 times longer T_1 relaxation time. Therefore contributions from the impurity phase Rb_6C_{60} are saturated and not visible in the spectra and relaxation rates.

The static ^{13}C NMR measurements were performed with a homebuilt spectrometer operating at a ^{13}C frequency of 83.7 MHz. Spectra were recorded by a spin-echo pulse sequence with four phase alternation. At high temperatures T_1 was measured by a conventional inversion recovery pulse sequence with echo detection, whereas at low temperatures the saturation recovery technique was applied. T_2 was measured by a Hahn echo sequence, which implies that only homonuclear dipolar couplings contribute to T_2 in addition to motional dynamics, whereas static heteronuclear couplings are canceled.

III. RESULTS AND DISCUSSION

A. Line shift

The ^{13}C line in Rb_4C_{60} is appreciably paramagnetically shifted to 182 ppm with respect to TMS at room temperature in accordance with Ref. 6. This shift is about identical to the one observed in K_4C_{60} and only 9 ppm smaller than the shift in superconducting Rb_3C_{60}. The temperature dependence of the total shift $\delta(T)$ (see Fig. 1) scales with the susceptibility $\chi_p(T)$,[13] demonstrating the existence of a paramagnetic Knight-shift contribution. The total shift is related to $\chi_p(t)$ by the following relation:

$$\underline{\underline{\delta}}(T)=\underline{\underline{\sigma}}+\underline{\underline{K}}(T)=\underline{\underline{\sigma}}+\chi_p(T)\underline{\underline{A}}\,\frac{1}{Ng_e\mu_B\gamma_N\mu_0}, \quad (3.1)$$

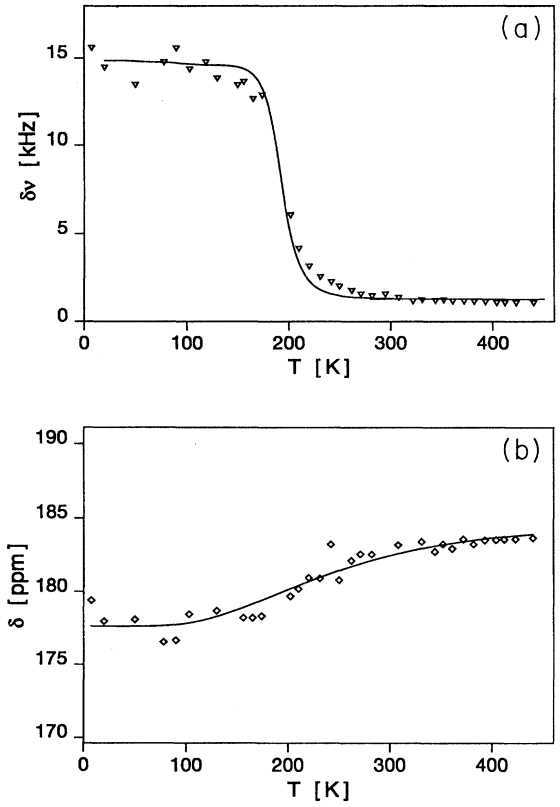

FIG. 1. ^{13}C line shift (b) and linewidth (a) in Rb_4C_{60} as function of temperature. The solid lines are simulations of the corresponding models as described in the text.

where $\chi_p(T)$ is modeled by a thermally activated electronic excitation.[13] The scenario behind this model can be summarized as follows. The degeneracy of the three t_{1u} derived bands is lifted by a Jahn-Teller distortion in such a way that the four electrons of C_{60}^{4-} are distributed on the two lower-lying t_{1u} bands, whereas the third (and empty) t_{1u} band is energetically split off by an energy ΔE_e. The ground state consists of filled bands and is therefore diamagnetic, although an appreciable van Vleck contribution to the susceptibility and the Knight shift is expected. With increasing temperature a thermal population of the third t_{1u} band proceeds giving rise to a thermally activated susceptibility. Since this band is most likely very narrow we expect strong localization of these electrons and therefore a Curie-like temperature dependence of their spin polarization. In summary this results in a temperature-dependent paramagnetic susceptibility $\chi_p(T)$ and corresponding Knight shift as

$$\chi_p(T)=\chi_0+\frac{C}{T}\frac{\nu_{\rm ex}e^{-\Delta E_e/2k_BT}}{\nu_0+\nu_{\rm ex}e^{-\Delta E_e/2k_BT}}, \qquad (3.2)$$

where χ_0 is a temperature-independent part and $\nu_{\rm ex}=2$, $\nu_0=4$ in the case of a twofold degenerate ground state. C is the Curie constant. A fit of this model to the shift data leads to an activation energy of 113 meV in agreement with susceptibility data. Using the temperature dependence of χ_p and δ, we can estimate the hyperfine coupling constant, which

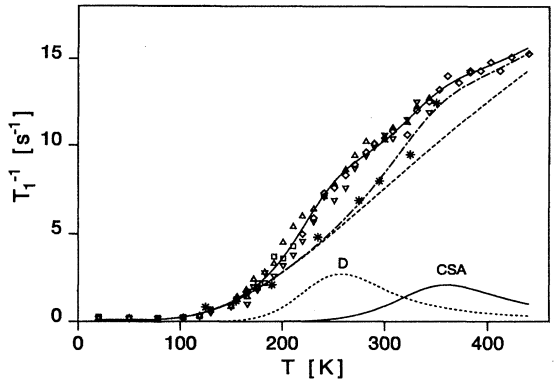

FIG. 2. Temperature dependence of the spin-lattice relaxation rate T_1^{-1} together with a simulation according to Eq. (3.3) (solid line). Data (*) taken from Ref. 17 were simulated with electronic (dashed line) and CSA relaxation (BPP peak, solid line) (– · – · –). The enriched sample shows an additional BPP peak due to homonuclear dipolar relaxation (BPP peak, dotted line) as described in the text.

amounts to $a_{\rm iso}=2\pi 0.7\times 10^6\ s^{-1}$. This value is smaller than in the A_3C_{60} compounds,[14] but comparable to the one observed in the high-temperature phase of A_1C_{60}.[15] The hyperfine coupling constant $a_{\rm iso}$ is expected to be small, because of the node of the p_z wave function of the carbons. Nevertheless, it is not zero as has been observed in other organic conductors.[16] The reason for this is not the nonplanar structure of C_{60}, as is sometimes argued, but the core polarization effect of the $2s$ electrons. We close the discussion of the Knight shift by noting that the electronic excitation which is visible in the Knight shift will appear again in the discussion of the T_1 relaxation.

B. T_1 relaxation

The complete temperature dependence of the T_1^{-1} relaxation rate is shown in Fig. 2. The stars are data taken from Ref. 17, which result from a nonenriched sample. There is an obvious discrepancy between the two data sets in the temperature range 200–300 K. It is interesting to note that results on K_4C_{60} with natural abundance of ^{13}C,[8] which was prepared under the same conditions as the enriched Rb_4C_{60} sample, exhibit an overall agreement with Ref 17. We are therefore led to assume that an additional relaxation path occurs due to homonuclear dipolar relaxation in the 10% enriched sample. This is also in agreement with the field dependence observed when comparing the data presented here (7.8 T) with those from Ref. 18 (9 T). We therefore expect to have the following contributions to the T_1^{-1} relaxation rate:

$$\frac{1}{T_1}=\frac{1}{T_{10}}+\frac{1}{T_{1L}}+\frac{1}{T_{1D}}+\frac{1}{T_{1\rm el}}, \qquad (3.3)$$

where contributions from molecular reorientation are represented by T_{1L}^{-1} and T_{1D}^{-1} and where $T_{1\rm el}^{-1}$ represents the contribution due to the electronic excitation. In T_{1D}^{-1} we summarize the contribution which is mainly due to fluctuating ^{13}C

TABLE I. Rotational parameters for Rb_4C_{60}. τ_{c0} is the reorientational correlation time for $T\to\infty$, ΔE the corresponding activation energy. T^* denotes the peak temperature, which is determined experimentally in a magnetic field of 7.8 T.

Mode detected by	T_1, K_4C_{60}	T_1, Rb_4C_{60}	T_2, K_4C_{60}	T_2, Rb_4C_{60}
τ_{c0L}	10^{-12} s	10^{-12} s	10^{-10} s	10^{-10} s
ΔE_L	180 meV	233 meV	160 meV	215 meV
T^*	280 K	350 K	145 K	190 K
τ_{c0D}		10^{-12} s		
ΔE_D		153 meV		

dipole-dipole interaction, whereas T_{1L}^{-1} is mainly caused by fluctuating shift anisotropy, where both are due to molecular reorientation. In addition we have introduced a temperature-independent background relaxation rate T_{10}^{-1}. T_{10}^{-1} amounts in our case to 0.1 s^{-1} which is quite small compared with the other relaxation rates. This background becomes visible at low temperatures, where all other mechanism cease. It is most likely caused by paramagnetic impurities.

1. CSA relaxation due to reorientational motion

Let us first discuss the relaxation time T_{1L} caused by fluctuating local fields, expressed by the second moment $\Delta\omega_L^2=\gamma^2\Delta B_L^2$ due to the reorientational motion of the C_{60}^{4-} molecules. The anisotropic chemical and paramagnetic shifts, summarized here as chemical shift anisotropy (CSA) at the local ^{13}C site, leads to a variation of the local field when the molecule reorients. The degree of fluctuation $\Delta\omega_L^2$ will depend on the details of the isotropic or anisotropic molecular reorientation, but will never exceed the total shift anisotropy. Since the details of the reorientation are not known it will serve as an adjustable parameter here. The corresponding spin-lattice relaxation rate can be readily expressed as[19,20]

$$\frac{1}{T_{1L}}=\frac{6}{40}\Delta\omega_L^2\frac{2\tau_{cL}}{1+\omega_0^2\tau_{cL}^2}, \tag{3.4}$$

where ω_0 is the Larmor frequency. Note that this relaxation rate increases proportional to B_0^2 for $\omega_0\tau_{cL}\ll 1$ and becomes field independent for $\omega_0\tau_{cL}\gg 1$. A peak in the relaxation rate is expected according to Bloembergen, Purcell, and Pound[20] (BPP) if $\omega_0\tau_{cL}=1$. The correlation time τ_{cL} is modeled here by a thermally activated process with activation energy ΔE_L:

$$\tau_{cL}=\tau_{cL0}\exp\left(\frac{\Delta E_L}{kT}\right). \tag{3.5}$$

The final parameters obtained from the data fitting are listed in Table I. The value obtained for $\Delta\omega_L=2\pi 13.7\times 10^3$ s^{-1} is in reasonable agreement with the CSA linewidth at low temperatures. The activation energy ΔE_L for this reorientational mode is obtained as 233 meV using an attempt frequency τ_{cL0} of 10^{-12} s. In a previous publication[8] we have shown that T_{1L} accounts sufficiently well for the reorientational motion of a non-enriched sample. It therefore holds also for the data shown in Ref. 17. In the enriched sample, the situation becomes more complicated: The reorientational motion should also lead to fluctuations of the dipole-dipole coupling between the ^{13}C nuclei. We therefore have to complement T_{1L} by the dipole-dipole contribution

$$\frac{1}{T_{1L}}=\frac{6}{40}\Delta\omega_L^2\frac{2\tau_{cL}}{1+\omega_0^2\tau_{cL}^2}+\frac{2}{3}(\Delta\omega_{D1})^2\left(\frac{\tau_{cL}}{1+\omega_0^2\tau_{cL}^2}+\frac{4\tau_{cL}}{1+4\omega_0^2\tau_{cL}^2}\right), \tag{3.6}$$

where $(\Delta\omega_{D1})^2$ represents the averaged second moment of the fluctuating dipole-dipole interaction. Its value was determined in the fitting procedure as $\Delta\omega_{D1}=2\pi 200$ s^{-1}, a rather small value. The reorientational part of the relaxation discussed here can therefore be described reasonably well by the first part which is also true for the data in Refs. 17 and 8. We note that similar relaxation peaks in T_1^{-1} were found in A_3C_{60}.[21,22]

2. Dipolar relaxation due to reorientational motion

Due to the enrichment of our compound, we observe an additional BPP maximum at lower temperatures, which is, comparing the enriched and the natural abundance samples, obviously enhanced by homonuclear dipolar couplings. This contribution is modeled by the additional term[19,20]

$$\frac{1}{T_{1,D}}=\frac{2}{3}(\Delta\omega_D)^2\left(\frac{\tau_{cD}}{1+\omega_0^2\tau_{cD}^2}+\frac{4\tau_{cD}}{1+4\omega_0^2\tau_{cD}^2}\right), \tag{3.7}$$

where $(\Delta\omega_D)^2$ and τ_{cD} are supposed to be different from the related parameters in Eq. (3.6). τ_{cD} is again assumed to exhibit a thermally activated temperature dependence. The following parameters were obtained in the fitting: $\tau_{c0D}=1\times 10^{-12}$ s, $\Delta E_D=157$ meV, and $\Delta\omega_D=2\pi 5.5\times 10^3$ s^{-1}. This contribution is also plotted separately in Fig. 2 like the CSA contribution.

C. Hyperfine relaxation caused by electronic excitation

It is obvious from Fig. 2 that the steady increase of T_1^{-1} with temperature cannot be accounted for by BPP-like relaxation expressions as discussed so far. In fact, it is expected that the paramagnetic contribution to the Knight shift and susceptibility which was discussed in Sec. III A results in an additional relaxation mechanism. If we adopt here the same model of a thermal excitation to a delocalized spin state, we expect to obtain the following expression for the electronic contribution to the relaxation rate:[23]

$$\frac{1}{T_{1\mathrm{el}}} = \hbar k_B T \Delta\omega_{\mathrm{el}}^2 \frac{\bar{\chi}_p}{\Gamma}, \tag{3.8}$$

where $\Delta\omega_{\mathrm{el}}^2$ is the second moment of the hyperfine interaction including isotropic and anisotropic parts. We have replaced the wave-vector-dependent dynamic susceptibility by the expression $\bar{\chi}_p/\Gamma$ which takes the density of excited states, i.e., the concentration of excited electrons into account as well as their scattering rate Γ.[23] The normalized and averaged susceptibility $\bar{\chi}_p$, which corresponds to the usual single-particle susceptibility divided by $g^2\mu_B^2$, can be written as

$$\bar{\chi}_p = \frac{1}{4k_BT} \frac{\nu_{\mathrm{ex}} e^{-\Delta E_e/2k_BT}}{\nu_0 + \nu_{\mathrm{ex}} e^{-\Delta E_e/2k_BT}}, \tag{3.9}$$

similar to the expression used for the Knight shift. $\bar{\chi}_p$ is given here in units of *energy*$^{-1}$ which together with the scattering rate Γ, given in units of energy, fulfills the unit requirements of Eq. (3.8) and results in the final expression

$$\frac{1}{T_{1\mathrm{el}}} = \Delta\omega_{\mathrm{el}}^2 \frac{\hbar}{4\Gamma} \frac{\nu_{\mathrm{ex}} e^{-\Delta E_e/2k_BT}}{\nu_0 + \nu_{\mathrm{ex}} e^{-\Delta E_e/2k_BT}}. \tag{3.10}$$

The dominant temperature dependence of $T_{1\mathrm{el}}$ derives from the last factor. We find from fitting Eq. (3.10) to the relaxation data that a satisfactory fit can be obtained without assuming any temperature dependence of Γ. The activation energy ΔE_e is found to be 104 meV. Within the accuracy of the experiment, the same value is observed in K_4C_{60},[8] indicating that this electronic excitation process is not directly influenced by the rotational dynamics of C_{60}^{4-}. By assuming $\Delta\omega_{\mathrm{el}} = 2\pi 10^7$ s^{-1}, a typical value for the hyperfine interaction which includes the anisotropic interactions in A_3C_{60},[14] we deduce a scattering rate $\Gamma/\hbar$ of about 10^{13} s^{-1}.

An alternative description of the relaxation rate is discussed by Kerkoud *et al.*[18] where the excitation across the band gap of an indirect semiconductor is considered. Again the band gap appears as an activation energy. These authors have investigated in addition the pressure dependence of this gap which seems too close under large enough pressure. At ambient pressure we find a better agreement of our experimental data with the relaxation expressions presented here. Another alternative would be an excitation to a local molecular high-spin (triplet) state. This would result in a very efficient relaxation mechanism which would again be thermally activated. However, this would lead to inhomogeneous relaxation throughout the sample, which is not observed and could in addition not explain the temperature-dependent Knight shift.

The combined thermal activation of the Knight shift and the relaxation rate leads to the conclusion that the excited electronic spins are delocalized. This does not necessarily imply, however, that they are charged and lead to conduction. Because of the expected extremely narrow bands and an appreciable electron-electron repulsion, characterized by the Hubbard U,[24,25] the A_4C_{60} compounds may be considered as Mott-Hubbard insulators. Jahn-Teller[26] and/or crystal-field effects might further split the ground state and lead to a highly correlated excited state. The observations discussed here as well as the pressure dependence of the T_1 relaxation[18] are in qualitative agreement with the prediction of this scenario, although the details will still have to be worked out.

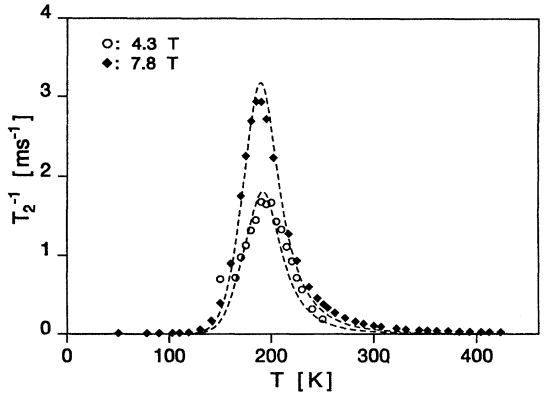

FIG. 3. Temperature dependence of the spin-spin relaxation rate T_2^{-1} at different magnetic fields. The quasi-temperature-independent background is already subtracted. The dashed line is a simulation of the reorientational contribution to T_2^{-1}.

D. Linewidth and T_2 relaxation

So far we have discussed T_1 relaxation which is sensitive to fluctuating local fields on a typical time scale of about $\omega_0^{-1} = 2\times10^{-9}$ s. The motional narrowing of the linewidth above 250 K clearly indicates that the C_{60} rotational motion changes in the temperature region 100–250 K on a time scale of about 3×10^{-5} s. The influence of rotational motion on the temperature-dependent linewidth $\delta\omega(T)$ can be described by the following implicit equation:[19]

$$(\delta\omega)^2 = (\delta\omega'')^2 + (\delta\omega')^2 \frac{2}{\pi} \arctan[\alpha\delta\omega\tau_{cS}(T)]. \tag{3.11}$$

We label the correlation time τ_{cS} of this motion by the subscript S in order to distinguish it formally from the motional modes discussed so far. It might originate from a different type of motion which does not contribute significantly to the T_1 relaxation. Again we assume that τ_{cS} is thermally activated with an activation energy ΔE_S, reflecting the rotational barrier between different molecular orientations. $\delta\omega''$ is the linewidth at high temperatures, $\delta\omega'$ the rigid lattice value. Using an attempt frequency of $\tau_{cS0}^{-1} = 10^{10}$ s^{-1} a linewidth calculation (Fig. 1) results in an activation energy $\Delta E_S = 220$ meV. We note that the activation energy depends rather sensitively on the attempt frequency. For example, if we choose an attempt frequency of $\tau_{cS0}^{-1} = 10^9$ s^{-1} an activation energy $\Delta E_S = 190$ meV is obtained. Before discussing these details any further we turn to the T_2 relaxation time which is also sensitive to slow motion and should reflect the same reorientational dynamics as the line narrowing. A peak in T_2^{-1} appears around 190 K. In Fig. 3, the T_2^{-1} relaxation rate is shown for two different fields as a function of temperature. At a static magnetic field of 4.3 T the decay is

almost monoexponential over the temperature range measured. At 7.8 T we use the initial slope of the decay function as a measure of T_2^{-1} since the magnetization curve does not show a monoexponential decay. This nonexponential behavior varies with temperature and is probably caused by the powder average of the anisotropic molecular reorientation.

In order to model the T_2^{-1} relaxation rate we apply the following relation:[19]

$$\frac{1}{T_2}=\frac{1}{40}\Delta\omega_{SC}^2[3J(\omega_0)+4J(0)]+\frac{1}{10}\frac{\Delta\omega_{SD}^2\tau_c}{1+\Delta\omega_{SD}^2\tau_c^2}. \tag{3.12}$$

The spectral density $J(\omega_0)$ is usually given by

$$J(\omega_0)=\frac{2\tau_c}{1+\omega_0^2\tau_c^2}, \tag{3.13}$$

whereas $J(0)$ is modeled by[27]

$$J(0)=\frac{2\tau_c}{1+\Delta\omega_{SC}^2\tau_c^2}, \tag{3.14}$$

which interpolates between the slow motion ($\Delta\omega_{SC}\tau_{cS}\gg 1$) and the extreme motional narrowing case ($\Delta\omega_{SC}\tau_{cS}\ll 1$). $\Delta\omega_{SC}^2$ is the second moment of the chemical shift frequency fluctuations caused by the reorientational process, whereas $\Delta\omega_{SD}^2$ is the corresponding fluctuating dipolar field. One of the essential differences between these two types of relaxation processes is their magnetic field dependence: $\Delta\omega_{SC}^2 \propto \gamma^2 B_0^2$ is a function of the static magnetic field, whereas $\Delta\omega_{SD}^2$ is field independent. We assume that τ_{cS} represents the correlation time of a thermally activated process as before. A reasonable fit of the experimental data is obtained with the parameters $\Delta\omega_{SC}=2\pi 4.8\times 10^3$ s^{-1} (7.8 T), $\Delta\omega_{SD}=2\pi 1.2\times 10^3$ s^{-1} as shown in Fig. 3 (dotted lines), where an attempt frequency of $\tau_{cS0}^{-1}=10^{10}$ s was used resulting in an activation energy of 210–220 meV (see also Table I). In addition to the relaxation processes caused by the molecular reorientation we must take the static dipole-dipole interaction into account. The T_2 relaxation caused by this interaction is quasitemperature independent above 250 K and below 130 K and was subtracted in Fig. 3 from the raw data.

In comparison to the nonenriched K_4C_{60}, which exhibits a T_2 relaxation time of 12.8 ms at room temperature, the relaxation rate of Rb_4C_{60} (10% ^{13}C) is enhanced [T_2(RT) = 4.27 ms]. This fact can be explained by intermolecular homonuclear dipolar couplings.[21] We model this part of T_2 by the corresponding second moment, which for a powder can be expressed as[19]

$$M_{2II}=\frac{\mu_0^2}{16\pi^2}\frac{3}{5}\gamma_I^4\hbar^2 I(I+1)f\sum_k\frac{1}{r_{jk}^6}. \tag{3.15}$$

The sum runs over all lattice sites occupied by carbon atoms. The factor f weights the sum corresponding to the statistical occupation by ^{13}C. At room temperature the C_{60}^{4-} molecules are rapidly rotating in Rb_4C_{60} as follows from our analysis. Since the rotational rate is much larger than the intramolecular ^{13}C-^{13}C interaction, this interaction vanishes on the average. However, intermolecular ^{13}C-^{13}C interaction is still operative and leads to an enhanced T_2 relaxation which we calculate by applying $T_2^{-1}=\sqrt{M_{2II}}$. For the calculation of the lattice sum we approximate the C_{60} molecules as points at the appropriate lattice sites. This is justified approximately by the rapid rotation. We obtain $T_2=12.1$ ms for natural abundance ^{13}C and $T_2=4.0$ ms for the 10% ^{13}C enriched sample. Both values are in good agreement with the experiment. At low temperatures, where the C_{60} rotation is frozen, the ^{13}C-^{13}C dipolar coupling is enhanced leading to an enhanced contribution to T_2.

E. Summary

In Table I we have listed the rotational parameters of Rb_4C_{60} separately for T_1 and T_2 derived motional dynamics. In order to gain some insight into the problem whether the T_2 and T_1 derived modes are different or not let us look at the details of the motional parameters. One could argue that the differences in the activation energies and correlation times are within experimental error and only a single motional mode is present. This would be very unusual since the comparison of different fullerides[21,22] shows a rather complex behavior. Similar rotational modes are observed for the A_3C_{60} and A_4C_{60} compounds although their crystal structure is different. In both cases, the Rb compounds show larger activation energies of T_1 and T_2 derived modes. The striking difference is that in the A_4C_{60} compounds the rotational mode visible in T_1 has more or less the same activation energy as the one observed in T_2 measurements in contrast to A_3C_{60} where they differ considerably. In these compounds, the energy barriers for uniaxial rotation and flipping of this rotation axis are thought to be clearly separated. In Ref. 28, the slow motion in K_3C_{60} (as observed by T_2 relaxation) was attributed to small angle reorientations. In A_4C_{60} this separation of energy scales is not observed. In contrast, the activation energy observed in the T_2^{-1} relaxation is about the same as the one derived from the T_1^{-1} relaxation. However, the attempt frequencies τ_{c0}^{-1} are quite different leading to different correlation times. A possible origin for these differences could be due to a more axial molecular hoping leading to the T_1 relaxation in contrast to a more isotropic highly correlated molecular reorientation causing line narrowing and T_2 relaxation. Further investigations are needed to solve this discrepancy.

Concerning the electronic excitation it is remarkable that about the same excitation energy is obtained for Rb_4C_{60} and K_4C_{60}. Our value determined from shift and T_1 measurements is, however, considerably lower than the 300 meV obtained from the analysis of μSR experiments[9] but in agreement with Raman results[7] and susceptibility measurements.[13]

IV. CONCLUSIONS

In summary we have shown that Rb_4C_{60} and K_4C_{60} are very similar in electronic structure and reorientational dynamics of the C_{60}^{4-} ions. The activation energies for reori-

entation are slightly smaller in K_4C_{60} compared with Rb_4C_{60}. Both compounds show a paramagnetic shift at low temperatures indicative of a van Vleck paramagnetic contribution and a thermal excitation across an electronic gap around 100 meV.

ACKNOWLEDGMENTS

We would like to acknowledge financial support by the Fonds der Chemischen Industrie and the Deutsche Forschungsgemeinschaft.

[1] S. Pekker, L. Forró, L. Milhály, and A. Jánossy, Solid State Commun. **90**, 349 (1994).
[2] J. H. Weaver, J. Phys. Chem. Solids **53**, 1433 (1992).
[3] P. J. Benning, D. M. Poirier, T. R. Ohno, Y. Chen, M. B. Jost, F. Stepniak, G. H. Kroll, J. H. Weaver, J. Fure, and R. E. Smalley, Phys. Rev. B **45**, 6899 (1992).
[4] M. de Seta and F. Evangelisti, Phys. Rev. Lett. **71**, 2477 (1993).
[5] Y. Iwasa, S. Watanabe, T. Kaneyasu, T. Yasuda, T. Koda, M. Nagata, and N. Mizutani, J. Phys. Chem. Solids **54**, 1795 (1993).
[6] D. W. Murphy, M. J. Rosseinsky, R. M. Fleming, R. Tycko, A. P. Ramirez, R. C. Haddon, T. Siegrist, G. Dabbagh, J. C. Tully, and R. E. Walstedt, J. Phys. Chem. Solids **53**, 1321 (1992).
[7] G. Ruani, P Guptasarma, and C Taliani, *Proceedings of the M^2S HTSC IV* [Physica C **235-240**, 2477 (1994)].
[8] G. Zimmer, M. Helmle, F. Rachdi, and M. Mehring, Europhys. Lett. **27**, 543 (1994).
[9] R. F. Kiefl, L. T. Duty, J. W. Schneider, A. MacFarlane, K. Chow, J. W. Elzey, P. Mendels, G. D. Morris, J. H. Brewer, E. J. Ansaldo, C. Niedermayer, D. R. Noakes, C. E. Stronach, B. Hitti, and J. E. Fischer, Phys. Rev. Lett. **69**, 2005 (1992).
[10] R. M. Fleming, M. J. Rosseinsky, A. P. Ramirez, D. W. Murphy, J. C. Tully, R. C. Haddon, T. Siegrist, R. Tycko, S. H. Glarum, P. Marsh, G. Dabbagh, S. M. Zahurak, A. V. Makhija, and C. Hampton, Nature **352**, 701 (1991).
[11] M. J. Rosseinsky, A. P. Ramirez, S. H. Glarum, D. W. Murphy, R. C. Haddon, A. F. Hebbard, T. T. M. Palstra, A. R. Kortan, S. M. Zahurak, and A. V. Makhija, Phys. Rev. Lett. **66**, 2830 (1991).
[12] A. F. Hebard, M. J. Rosseinsky, R. C. Haddon, D. W. Murphy, S. H. Glarum, T. T. M. Palstra, A. P. Ramirez, and A. R. Kortan, Nature **350**, 600 (1991).
[13] I. Lukyanchuk, N. Kirova, F. Rachdi, C. Goze, P. Molinie, and M. Mehring, Phys. Rev. B **51**, 3978 (1995).
[14] M. Mehring, F. Rachdi, and G. Zimmer, Philos. Mag. **70**, 787 (1994).
[15] R. Tycko, G. Dabbagh, D. W. Murphy, Q. Zhu, and J. E. Fischer, Phys. Rev. B **48**, 9097 (1993).
[16] K. F. Thier and M. Mehring, Phys. Rev. B **50**, 2142 (1994).
[17] R. Tycko, J. Phys. Chem. Solids **54**, 1713 (1993).
[18] R. Kerkoud, P. Auban-Senzier, D. Jerome, S. Brazovskii, I. Lukyanchuk, N. Kirova, F. Rachdi, C. Goze, P. Bernier (unpublished).
[19] A. Abragam, *Principles of Nuclear Magnetism* (Oxford Science, New York, 1989).
[20] N. Bloembergen, E. M. Purcell, and R. V. Pound, Phys. Rev. **73**, 679 (1948).
[21] Y. Yoshinari, H. Alloul, G. Kriza, and K. Holczer, Phys. Rev. Lett. **71**, 2413 (1993).
[22] G. Zimmer, M. Mehring, and F. Rachdi (unpublished).
[23] M. Mehring, Appl. Mag. Reson. **3**, 383 (1992).
[24] J. P. Lu, Phys. Rev. B **49**, 5687 (1994).
[25] R. W. Lof, M. A. van Veenendaal, B. Koopmans, H. T. Jonkman, and G. A. Sawatzky, Phys. Rev. Lett. **68**, 3924 (1992).
[26] N. Manini, E. Tosatti, and A. Auerbach, Phys. Rev. B **49**, 13 008 (1994).
[27] J. Rautter, A. Grupp, M. Mehring, J. Alexander, K. Müllen, and W. Huber, Mol. Phys. **76**, 37 (1992).
[28] S. E. Barrett and R. Tycko, Phys. Rev. Lett. **69**, 3754 (1992).